

Genomic insights into the origin of farming in the ancient Near East

Iosif Lazaridis^{1,2}, Dani Nadel³, Gary Rollefson⁴, Deborah C. Merrett⁵, Nadin Rohland¹, Swapna Mallick^{1,2,6}, Daniel Fernandes^{7,8}, Mario Novak^{7,9}, Beatriz Gamarra⁷, Kendra Sirak^{7,10}, Sarah Connell⁷, Kristin Stewardson^{1,6}, Eadaoin Harney^{1,6,11}, Qiaomei Fu^{1,12,13}, Gloria Gonzalez-Fortes¹⁴, Eppie R. Jones¹⁵, Songül Alpaslan Roodenberg¹⁶, György Lengyel¹⁷, Fanny Bocquentin¹⁸, Boris Gasparian¹⁹, Janet M. Monge²⁰, Michael Gregg²⁰, Vered Eshed²¹, Ahuva-Sivan Mizrahi²¹, Christopher Meiklejohn²², Fokke Gerritsen²³, Luminita Bejenaru²⁴, Matthias Blüher²⁵, Archie Campbell²⁶, Giampiero Cavalleri²⁷, David Comas²⁸, Philippe Froguel^{29,30}, Edmund Gilbert²⁷, Shona M. Kerr²⁶, Peter Kovacs³¹, Johannes Krause³², Darren McGettigan³³, Michael Merrigan³⁴, D. Andrew Merriwether³⁵, Seamus O'Reilly³⁴, Martin B. Richards³⁶, Ornella Semino³⁷, Michel Shamoony-Pour³⁵, Gheorghe Stefanescu³⁸, Michael Stumvoll²⁵, Anke Tönjes²⁵, Antonio Torroni³⁷, James F. Wilson^{39,40}, Loic Yengo²⁹, Nelli A. Hovhannisanian⁴¹, Nick Patterson², Ron Pinhasi⁷ & David Reich^{1,2,6}

We report genome-wide ancient DNA from 44 ancient Near Easterners ranging in time between ~12,000 and 1,400 BC, from Natufian hunter-gatherers to Bronze Age farmers. We show that the earliest populations of the Near East derived around half their ancestry from a 'Basal Eurasian' lineage that had little if any Neanderthal admixture and that separated from other non-African lineages before their separation from each other. The first farmers of the southern Levant (Israel and Jordan) and Zagros Mountains (Iran) were strongly genetically differentiated, and each descended from local hunter-gatherers. By the time of the Bronze Age, these two populations and Anatolian-related farmers had mixed with each other and with the hunter-gatherers of Europe to greatly reduce genetic differentiation. The impact of the Near Eastern farmers extended beyond the Near East: farmers related to those of Anatolia spread westward into Europe; farmers related to those of the Levant spread southward into East Africa; farmers related to those of Iran spread northward into the Eurasian steppe; and people related to both the early farmers of Iran and to the pastoralists of the Eurasian steppe spread eastward into South Asia.

Between 10,000 and 9,000 BC, humans began practicing agriculture in the Near East¹. In the ensuing five millennia, plants and animals domesticated in the Near East spread throughout West Eurasia (a vast region that also includes Europe) and beyond. The relative homogeneity of present-day West Eurasians in a world context² suggests the possibility of extensive migration and admixture that homogenized geographically and genetically disparate sources of ancestry. The spread of the world's first farmers from the Near East would have been a mechanism for such homogenization. To date, however, owing to the poor preservation of DNA in warm climates, it has been impossible to study the population structure and history of the first farmers and to trace their contribution to later populations.

In order to overcome the obstacle of poor DNA preservation, we took advantage of two methodological developments. First, we sampled from the inner ear region of the petrous bone^{3,4} which can yield up to ~100 times more endogenous DNA than other skeletal elements⁴. Second, we used in-solution hybridization⁵ to enrich extracted DNA for about 1.2 million single nucleotide polymorphism (SNP) targets^{6,7}, making efficient sequencing practical by filtering out microbial and non-informative human DNA. We merged all sequences extracted from each individual, and randomly sampled a single sequence with minimum mapping and sequence quality to represent each SNP, restricting our investigation to individuals with at least 9,000 SNPs covered at least once (Methods). We obtained genome-wide data that passed

¹Department of Genetics, Harvard Medical School, Boston, Massachusetts 02115, USA. ²Broad Institute of MIT and Harvard, Cambridge, Massachusetts 02142, USA. ³The Zinman Institute of Archaeology, University of Haifa, Haifa 3498838, Israel. ⁴Department of Anthropology, Whitman College, Walla Walla, Washington 99362, USA. ⁵Department of Archaeology, Simon Fraser University, Burnaby, British Columbia V5A 1S6, Canada. ⁶Howard Hughes Medical Institute, Harvard Medical School, Boston, Massachusetts 02115, USA. ⁷School of Archaeology and Earth Institute, Belfield, University College Dublin, Dublin 4, Ireland. ⁸CIAS, Department of Life Sciences, University of Coimbra, Coimbra 3000-456, Portugal. ⁹Institute for Anthropological Research, Zagreb 10000, Croatia.

¹⁰Department of Anthropology, Emory University, Atlanta, Georgia 30322, USA. ¹¹Department of Organismic and Evolutionary Biology, Harvard University, Cambridge, Massachusetts 02138, USA.

¹²Department of Evolutionary Genetics, Max Planck Institute for Evolutionary Anthropology, Leipzig 04103, Germany. ¹³Key Laboratory of Vertebrate Evolution and Human Origins of Chinese Academy of Sciences, IVPP, CAS, Beijing 100044, China. ¹⁴Department of Biology and Evolution, University of Ferrara, Ferrara I-44121, Italy. ¹⁵Department of Zoology, University of Cambridge, Cambridge CB2 3EJ, UK. ¹⁶J.M. van Nassauw-Noord 2071 VA, The Netherlands. ¹⁷Department of Prehistory and Archaeology, University of Miskolc, Miskolc-Egyetemváros 3515, Hungary. ¹⁸French National Centre for Scientific Research, UMR 7041, Nanterre Cedex 92023, France. ¹⁹Institute of Archaeology and Ethnology, National Academy of Sciences of the Republic of Armenia, Yerevan 0025, Republic of Armenia. ²⁰University of Pennsylvania Museum of Archaeology and Anthropology, Philadelphia, Pennsylvania 19104, USA. ²¹Israel Antiquities Authority, Jerusalem 91004, Israel. ²²Department of Anthropology, University of Winnipeg, Winnipeg, Manitoba R3B 2E9, Canada. ²³Netherlands Institute in Turkey, Istanbul 34433, Turkey. ²⁴Faculty of Biology, Alexandru Ioan Cuza University of Iasi, Iasi 700505, Romania. ²⁵Department of Internal Medicine and Dermatology, Clinic of Endocrinology and Nephrology, Leipzig 04103, Germany.

²⁶Generation Scotland, Centre for Genomic and Experimental Medicine, MRC Institute of Genetics and Molecular Medicine, University of Edinburgh, Western General Hospital, Edinburgh EH4 2XU, UK.

²⁷RCSI Molecular & Cellular Therapeutics, Royal College of Surgeons in Ireland, Dublin 2, Ireland. ²⁸Institut de Biología Evolutiva (CSIC-UPF), Departament de Ciències Experimentals i de la Salut, Universitat Pompeu Fabra, Barcelona 08003, Spain. ²⁹Univ. Lille, CNRS, Institut Pasteur de Lille, UMR 8199 - EGIS, Lille F-59000, France. ³⁰Imperial College London, Department of Genomics of Common Disease, London Hammersmith Hospital, London W12 0HS, UK. ³¹Leipzig University Medical Center, IfB Adiposity Diseases, Leipzig 04103, Germany. ³²Max Planck Institute for the Science of Human History, Jena 07745, Germany. ³³School of History, Newman Building, University College Dublin, Belfield, Dublin 4, Ireland. ³⁴Genealogical Society of Ireland, Dún Laoghaire, County Dublin, Ireland. ³⁵Department of Anthropology, Binghamton University, State University of New York, New York 13902, USA. ³⁶Department of Biological Sciences, School of Applied Sciences, University of Huddersfield, Queensgate, Huddersfield HD1 3DH, UK. ³⁷Dipartimento di Biologia e Biotecnologie "L. Spallanzani", Università di Pavia, Pavia 27100, Italy. ³⁸Institutul de Cercetări Biologice, Iași 700505, Romania. ³⁹Usher Institute for Population Health Sciences and Informatics, University of Edinburgh, Edinburgh EH8 9AG, UK. ⁴⁰MRC Human Genetics Unit, MRC Institute of Genetics and Molecular Medicine, University of Edinburgh, Edinburgh EH4 2XU, UK. ⁴¹Center of Excellence in Applied Biosciences, Yerevan State University, Yerevan 0025, Republic of Armenia.

[§]These authors jointly supervised this work.

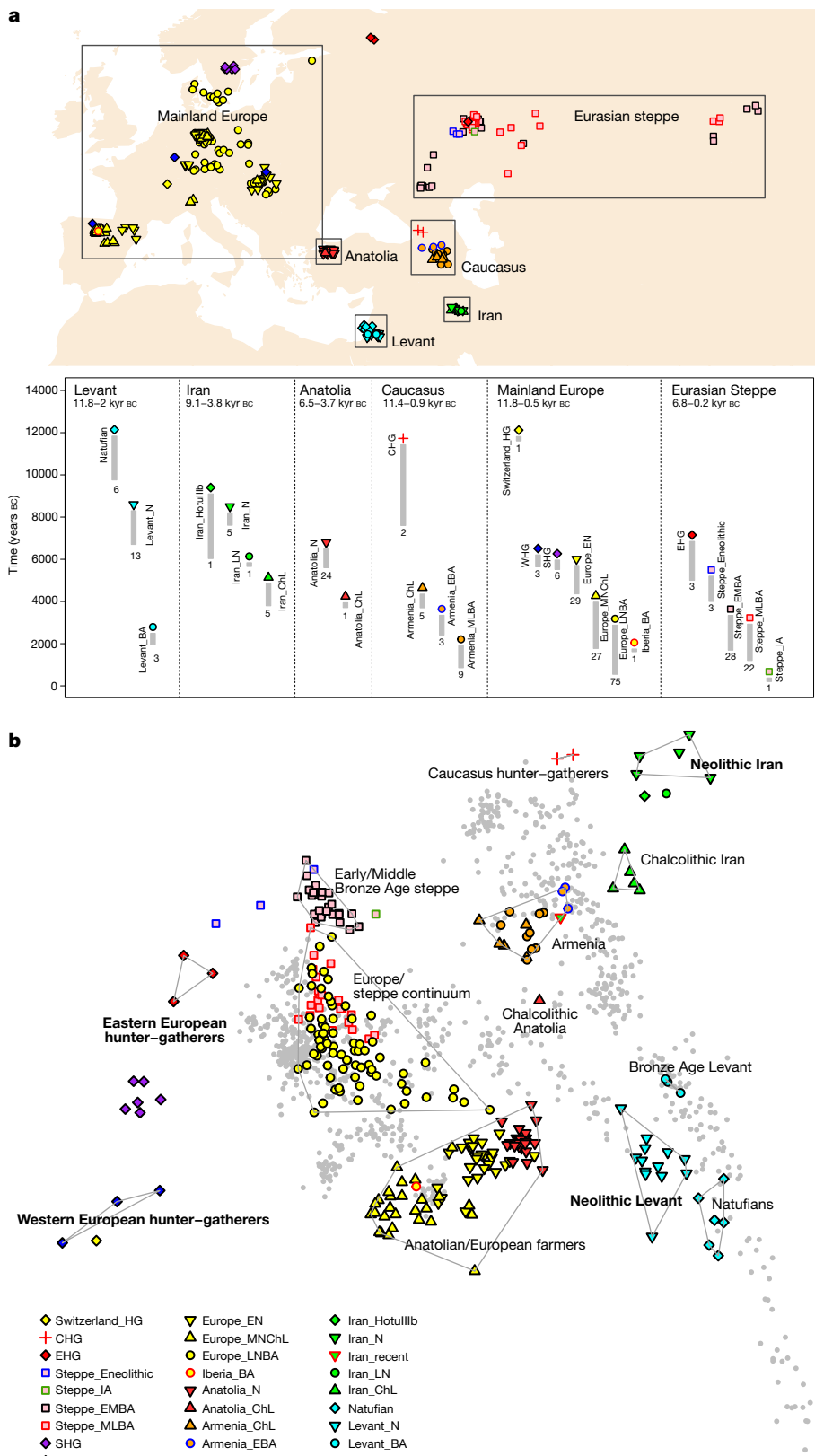


Figure 1 | Genetic structure of ancient West Eurasia. **a**, Sampling locations and times in six regions. Sample sizes for each population are given below each bar. E, Early; M, Middle; L, Late; HG, hunter-gatherer; N, Neolithic; ChL, Chalcolithic; BA, Bronze Age; IA, Iron Age. **b**, Principal components analysis of 991 present-day West Eurasians (grey points) with 278 projected ancient samples (excluding the Upper Palaeolithic Ust'-Ishim, Kostenki14, and MA1). To avoid visual clutter, population labels of present-day individuals are shown in Extended Data Fig. 1.

quality control for 45 individuals on whom we had a median coverage of 172,819 SNPs. We assembled direct radiocarbon dates on skeletal remains from 26 of these individuals (22 newly generated for this study) (Supplementary Table 1).

The newly reported ancient individuals date to ~12,000–1,400 bc and come from the southern Caucasus (Armenia), northwestern Anatolia (Turkey), Iran, and the southern Levant (Israel and Jordan) (Supplementary Table 1).

(Supplementary Table 1 and Fig. 1a). (One individual had a radiocarbon date that was not in agreement with the date of its archaeological context and was also a genetic outlier.) The samples include Epipalaeolithic Natufian hunter-gatherers from Raqefet Cave in the Levant (~12,000–9,800 BC); a likely Mesolithic individual (HotuIIIb) from Hotu Cave in the Alborz mountains of Iran (probable date of 9,100–8,600 BC); pre-pottery Neolithic farmers from ‘Ain Ghazal and

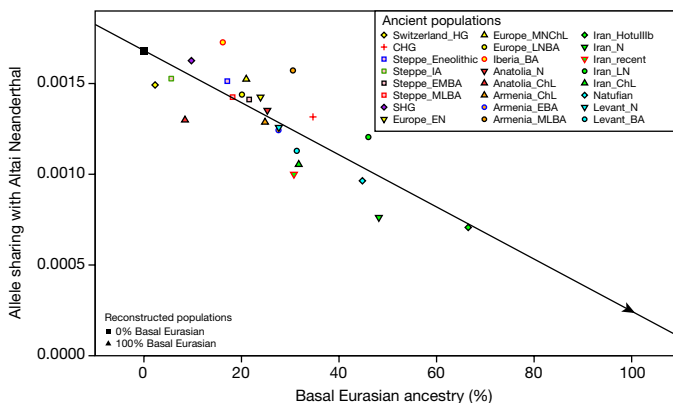


Figure 2 | Basal Eurasian ancestry explains the reduced Neanderthal admixture in West Eurasians. Basal Eurasian ancestry estimates are negatively correlated to a statistic measuring Neanderthal ancestry f_4 (*Test*, Mbuti; Altai, Denisovan).

Motza in the southern Levant (~8,300–6,700 BC); and early farmers from Ganj Dareh in the Zagros mountains of western Iran (~8,200–7,600 BC). The samples also include later Neolithic, Chalcolithic (~4,800–3,700 BC), and Bronze Age (~3,350–1,400 BC) individuals (Supplementary Information, section 1). We combined our data with previously published ancient data^{7–15} to form a dataset of 281 ancient individuals. We then further merged these data with 2,583 present-day people genotyped on the Affymetrix Human Origins array^{13,16} (238 newly generated) (Supplementary Table 2 and Supplementary Information, section 2). We grouped the ancient individuals on the basis of archaeological culture and chronology (Fig. 1a and Supplementary Table 1). We refined the grouping on the basis of patterns evident in Principal Components Analysis (PCA)¹⁷ (Fig. 1b and Extended Data Fig. 1), ADMIXTURE model-based clustering¹⁸ (Extended Data Fig. 2a), and ‘outgroup’ f_3 -analysis (Extended Data Fig. 3). We used f_4 -statistics to identify outlier individuals and to cluster phylogenetically indistinguishable groups into ‘Analysis Labels’ (Supplementary Information, section 3).

We analysed these data to address six questions. (1) Previous work has shown that the first European farmers harboured ancestry from a Basal Eurasian lineage that diverged from the ancestors of north Eurasian hunter-gatherers and East Asians before they separated from each other¹³. What was the distribution of Basal Eurasian ancestry in the ancient Near East? (2) Were the first farmers of the Near East part of a single homogeneous population, or were they regionally differentiated? (3) Was there continuity between late pre-agricultural hunter-gatherers and early farming populations, or were the hunter-gatherers largely displaced by a single expansive population, as in early Neolithic Europe?⁸ (4) What is the genetic contribution of these early Near Eastern farmers to later populations of the Near East? (5) What is the genetic contribution of the early Near Eastern farmers to later populations of mainland Europe, the Eurasian steppe, and to populations outside West Eurasia? (6) Do our data provide broader insights about population transformations in West Eurasia?

Basal Eurasian and Neanderthal ancestry

The ‘Basal Eurasians’ are a lineage hypothesized¹³ to have split off before the differentiation of all other Eurasian lineages, including eastern non-African populations such as the Han Chinese, and even the early diverged lineage represented by the genome sequence of the ~45,000-year-old Upper Palaeolithic Siberian from Ust'-Ishim¹¹. To test for Basal Eurasian ancestry, we computed the statistic f_4 (*Test*, Han; Ust'-Ishim, Chimp) (Supplementary Information, section 4), which measures the excess of allele sharing of Ust'-Ishim with a variety of *Test* populations compared to Han as a baseline. This statistic is significantly negative ($Z < -3.7$) for all ancient Near Easterners as well as Neolithic and later Europeans, consistent with them having ancestry from a deeply divergent

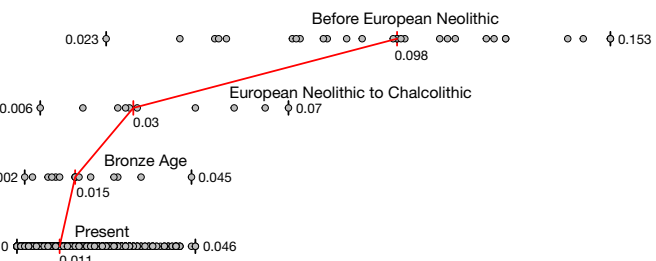


Figure 3 | Genetic differentiation and its marked decrease over time in West Eurasia. Pairwise F_{ST} distribution among populations belonging to four successive time slices in West Eurasia; the median (red) and range of F_{ST} is shown.

Eurasian lineage that separated from the ancestors of most Eurasians before the separation of Han and Ust'-Ishim. We used *qpAdm* (ref. 7) to estimate Basal Eurasian ancestry in each *Test* population. We obtained the highest estimates in the earliest populations from both Iran ($66 \pm 13\%$ in the likely Mesolithic sample, $48 \pm 6\%$ in Neolithic samples), and the Levant ($44 \pm 8\%$ in Epipalaeolithic Natufians) (Fig. 2), showing that Basal Eurasian ancestry was widespread across the ancient Near East.

West Eurasians harbour significantly less Neanderthal ancestry than East Asians^{19–21}, which could be explained if West Eurasians (but not East Asians) have partial ancestry from a source that diluted their Neanderthal inheritance²⁰. Supporting this theory, we observe a negative correlation between Basal Eurasian ancestry and the rate of shared alleles with Neanderthals¹⁹ (Supplementary Information, section 5 and Fig. 2). By extrapolation, we infer that the Basal Eurasian population had lower Neanderthal ancestry than non-Basal Eurasian populations and possibly none (95% confidence interval truncated at zero of 0–60%; Fig. 2; Methods). The finding of little if any Neanderthal ancestry in Basal Eurasians could be explained if the Neanderthal admixture into modern humans ~50,000–60,000 years ago¹¹ largely occurred after the splitting of the Basal Eurasians from other non-Africans.

It is striking that the highest estimates of Basal Eurasian ancestry are from the Near East, given the hypothesis that it was there that most admixture between Neanderthals and modern humans occurred^{19,22}. This could be explained if Basal Eurasians thoroughly admixed into the Near East before the time of the samples we analysed but after the Neanderthal admixture. Alternatively, the ancestors of Basal Eurasians may have always lived in the Near East, but the lineage of which they were a part did not participate in the Neanderthal admixture.

A population without Neanderthal admixture, basal to other Eurasians, may have plausibly lived in Africa. Craniometric analyses have suggested an affinity between the Natufians and populations of north or sub-Saharan Africa^{23,24}, a result that finds some support from Y chromosome analysis showing that the Natufians and successor Levantine Neolithic populations carried haplogroup E, likely to be of ultimately African origin, which has not been detected in other ancient males from West Eurasia^{7,8} (Supplementary Information, section 6). However, no affinity of Natufians to sub-Saharan Africans is evident in our genome-wide analysis, as present-day sub-Saharan Africans do not share more alleles with Natufians than with other ancient Eurasians (Extended Data Table 1). (We could not test for a link to present-day North Africans, who owe most of their ancestry to back-migration from Eurasia^{25,26}.) The idea of Natufians as a vector for the movement of Basal Eurasian ancestry into the Near East is also not supported by our data, as the Basal Eurasian ancestry in the Natufians ($44 \pm 8\%$) is consistent with stemming from the same population as that in the Neolithic and Mesolithic populations of Iran, and is not greater than in those populations (Supplementary Information, section 4). Further insight into the origins and legacy of the Natufians could come from comparison to Natufians from additional sites, and to ancient DNA from North Africa.

Extreme differentiation in the ancient Near East

PCA on present-day West Eurasian populations (Methods and Extended Data Fig. 1), on which we projected the ancient individuals

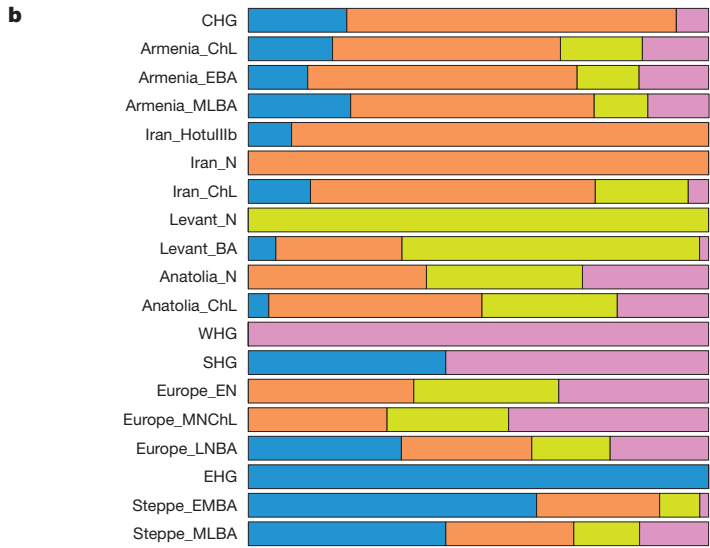
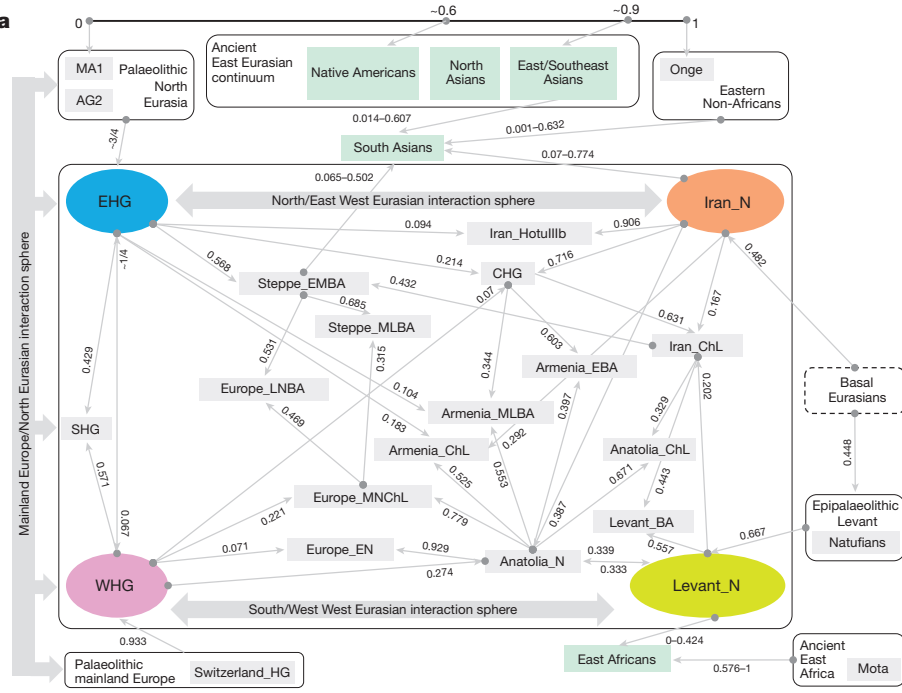


(Fig. 1b), replicates previous findings of a Europe–Near East contrast along the horizontal principal component 1 (PC1) and parallel clines (PC2) in both Europe and the Near East^{8,13} (Extended Data Fig. 1). Ancient samples from the Levant clustered at one end of the Near Eastern cline, and ancient samples from Iran at the other. The two Caucasus hunter-gatherers (CHG)⁹ are less extreme along PC1 than the Mesolithic and Neolithic individuals from Iran, while individuals from Chalcolithic Anatolia, Iran, Armenia, and Bronze Age Armenia occupy intermediate positions. Qualitatively, the PCA has the appearance of a quadrangle whose four corners are some of the oldest samples: bottom-left, Western hunter-gatherers (WHD); top-left, Eastern hunter-gatherers (EHG); bottom-right, Neolithic Levant and Natufians; top-right, Neolithic Iran. This suggests that diverse ancient West Eurasians can be modelled as mixtures of as few as four streams of ancestry related to these populations, which we confirmed using *qpWave* (ref. 7) (Supplementary Information, section 7).

We computed squared allele frequency differentiation between all pairs of ancient West Eurasians²⁷ (Methods; Fig. 3 and Extended Data Figs 2b and 4), and found that the populations at the four corners of

the quadrangle had differentiation of $F_{ST} = 0.08\text{--}0.15$, comparable to the value of 0.09–0.13 seen between present-day West Eurasians and East Asians (Han) (Supplementary Table 3). By contrast, by the Bronze Age, genetic differentiation between pairs of West Eurasian populations had reached its present-day low levels (Fig. 3): today, F_{ST} is ≤ 0.025 for 95% of the pairs of West Eurasian populations and ≤ 0.046 for all pairs (Supplementary Table 3). These results point to a demographic process that established high differentiation across West Eurasia and then reduced this differentiation over time.

Continuity between hunter-gatherers and early farmers

Our data document continuity across the transition between hunter-gatherers and farmers, separately in the southern Levant and in the southern Caucasus–Iran highlands. The qualitative evidence for this is that PCA, ADMIXTURE, and outgroup f_3 analysis cluster Levantine hunter-gatherers (Natufians) with Levantine farmers, and Iranian and CHG with Iranian farmers (Fig. 1b and Extended Data Figs 1, 3). We confirm this in the Levant by showing that its early farmers share significantly more alleles with Natufians than with the early farmers of Iran:

the statistic $f_4(\text{Levant_N}, \text{Chimp}; \text{Natufian}, \text{Iran_N})$ is significantly positive ($Z=13.6$). The early farmers of the Caucasus–Iran highlands similarly share significantly more alleles with the hunter–gatherers of this region than with the early farmers from the Levant: the statistic $f_4(\text{Iran_N}, \text{Chimp}; \text{Caucasus or Iran highland hunter-gatherers}, \text{Levant_N})$ is significantly positive ($Z>6$).

Admixture in the ancient Near East

Almost all ancient and present-day West Eurasians have evidence of significant admixture between two or more ancestral populations, as documented by statistics of the form $f_3(\text{Test}; \text{Reference}_1, \text{Reference}_2)$ which, if negative, show that a test population's allele frequencies tend to be an intermediate between two reference populations¹⁶ (Extended Data Table 2). To better understand the admixture history beyond these patterns, we used *qpAdm* (ref. 7), which can evaluate whether a particular test population is consistent with being derived from a set of proposed source populations, and if so, infer mixture proportions (Methods). We used this approach to carry out a systematic survey of ancient West Eurasian populations to explore their possible sources of admixture (Fig. 4 and Supplementary Information, section 7).

Among first farmers, those of the Levant trace approximately two-thirds of their ancestry to people related to Natufian hunter–gatherers and about one-third to people related to Anatolian farmers (Supplementary Information, section 7). Western Iranian first farmers cluster with the likely Mesolithic HotuIIb individual and more remotely with hunter–gatherers from the southern Caucasus (Fig. 1b), and share alleles at an equal rate with Anatolian and Levantine early farmers (Supplementary Information, section 7), highlighting the long-term isolation of western Iran.

During subsequent millennia, the early farmer populations of the Near East expanded in all directions and mixed, as we can model populations of the Chalcolithic and subsequent Bronze Age only as having ancestry from two or more sources. The Chalcolithic people of western Iran can be modelled as a mixture of the Neolithic people of western Iran, the Levant and CHG, consistent with their position in the PCA (Fig. 1b). Admixture from populations related to the Chalcolithic people of western Iran had a wide impact, consistent with contributing around 44% of the ancestry of Levantine Bronze Age populations in the south and about 33% of the ancestry of the Chalcolithic North-West Anatolians in the west. Our analysis shows that the ancient populations of Chalcolithic Iran, Chalcolithic Armenia, Bronze Age Armenia and Chalcolithic Anatolia were all composed of the same ancestral components, albeit in slightly different proportions (Fig. 4b and Supplementary Information, section 7).

Admixture into Europe, East Africa and South Asia

Admixture did not only occur within the Near East but also extended towards Europe. To the north, a population related to people of Chalcolithic Iran contributed about 43% of the ancestry of early Bronze Age populations of the steppe. The spread of Near Eastern ancestry into the Eurasian steppe was previously inferred⁷ without access to ancient samples, with a population related to present-day Armenians as a suggested source^{7,8}. To the west, the early farmers of mainland Europe were descended from a population related to Neolithic North-Western Anatolians⁸. This is consistent with an Anatolian origin of farming in Europe, but does not reject other sources, as the spatial distribution of the Anatolian/European-like farmer populations is unknown. We can rule out the hypothesis that European farmers stem directly from a population related to the ancient farmers of the southern Levant^{28,29}, however, because European farmers share more alleles with Anatolian Neolithic farmers than with Levantine farmers, as attested by the positive statistic $f_4(\text{Europe_EN}, \text{Chimp}; \text{Anatolia_N}, \text{Levant_N})$ ($Z=15$).

Migration from the Near East also occurred towards the southwest into East African populations, which experienced West Eurasian admixture around 1,000 BC^{30,31}. Previously, the West Eurasian population known to be the best proxy for this ancestry was present-day Sardinians³¹, who

resemble Neolithic Europeans genetically^{13,32}. However, our analysis shows that East African ancestry is significantly better modelled by Levantine early farmers than by Anatolian or early European farmers, implying that the spread of this ancestry to East Africa was not from the same group that spread Near Eastern ancestry into Europe (Extended Data Fig. 5 and Supplementary Information, section 8).

In South Asia, our dataset provides insight into the sources of Ancestral North Indians (ANI), a West Eurasian-related population that no longer exists in unmixed form but contributes a variable amount of the ancestry of South Asians^{33,34} (Supplementary Information, section 9 and Extended Data Fig. 5). We show that it is impossible to model the ANI as being derived from any single ancient population in our dataset. However, it can be modelled as a mix of ancestries related to both early farmers of western Iran and people of the Bronze Age Eurasian steppe; all sampled South Asian groups are inferred to have significant amounts of both ancestral types. The demographic impact of steppe-related populations on South Asia was substantial, as the Mala, a south Indian population with minimal ANI along the ‘Indian Cline’ of such ancestry^{33,34}, is inferred to have around 18% steppe-related ancestry, while the Kalash of Pakistan are inferred to have about 50%, similar to present-day northern Europeans⁷.

Population transformations in West Eurasia and beyond

We were concerned that our conclusions might be biased by the particular populations we happened to sample, and that we would have obtained qualitatively different conclusions without data from some key populations. We tested our conclusions by plotting the inferred position of admixed populations in PCA against a weighted combination of their inferred source populations and obtained qualitatively consistent results (Extended Data Fig. 6).

To further assess the robustness of our inferences, we developed a method to infer the existence and genetic affinities of ancient populations from unobserved ‘ghost’ populations (Supplementary Information, section 10 and Extended Data Fig. 7). This method takes advantage of the insight that if an unsampled ghost population admixes with differentiated ‘substratum’ populations, it is possible to extrapolate its identity by intersecting clines of populations with variable proportions of ghost and substratum ancestry. Applying this approach while withholding major populations, we validated some of our key inferences, successfully inferring mixture proportions consistent with those obtained when the populations were included in the analysis. Application of this method highlights the impact of Ancient North Eurasian (ANE) ancestry related to the ~22,000 BC Mal’ta 1 and ~15,000 BC Afontova Gora 2 (ref. 15) on populations living in Europe, the Americas and Eastern Eurasia. Eastern Eurasians can be modelled as arrayed along a cline with different proportions of ANE ancestry (Supplementary Information, section 11 and Extended Data Fig. 8), ranging from about 40% ANE in Native Americans, matching previous findings^{13,15}, to no less than around 5–10% ANE in diverse East Asian groups including Han Chinese (Extended Data Figs 5, 7f). We also document a cline of ANE ancestry across the East–West extent of Eurasia. Eastern hunter–gatherers (EHG) derive about three-quarters of their ancestry from the ANE (Supplementary Information, section 11); Scandinavian hunter–gatherers^{7,8,13} (SHG) are a mix of EHG and WHG; and WHG are a mix of EHG and populations related to the Upper Palaeolithic Bichon from Switzerland (Supplementary Information, section 7). Northwest Anatolians—with ancestry from a population related to European hunter–gatherers (Supplementary Information, section 7)—are better modelled if this ancestry is taken as more extreme than Bichon (Supplementary Information, section 10).

The population structure of the ancient Near East was not independent of that of Europe (Supplementary Information, section 4), as evidenced by the highly significant ($Z=-8.9$) statistic $f_4(\text{Iran_N}, \text{Natufian}; \text{WHG}, \text{EHG})$ which suggests gene flow in ‘northeastern’ (Neolithic Iran/EHG) and ‘southwestern’ (Levant/WHG) interaction spheres (Fig. 4d). This interdependence of the ancestry of Europe and

the Near East may have been mediated by unsampled geographically intermediate populations³⁵ that contributed ancestry to both regions.

Conclusions

By analysing genome-wide ancient DNA data from ancient individuals from the Levant, Anatolia, the southern Caucasus and Iran, we have provided a first glimpse into the demographic structure of the human populations that transitioned to farming. We reject the hypothesis that the spread of agriculture in the Near East was achieved by the dispersal of a single farming population displacing the hunter-gatherers they encountered. Instead, the spread of ideas and farming technology moved faster than the spread of people, as we can determine from the fact that the population structure of the Near East was maintained throughout the transition to agriculture. A priority for future ancient DNA studies should be to obtain data from older periods, which would reveal the deeper origins of the population structure in the Near East. It will also be important to obtain data from the ancient civilizations of the Near East to bridge the gap between the region's prehistoric inhabitants and those of the present.

Online Content Methods, along with any additional Extended Data display items and Source Data, are available in the online version of the paper; references unique to these sections appear only in the online paper.

Received 8 March; accepted 18 July 2016.

Published online 25 July 2016.

- Barker, G. & Goucher, C. *The Cambridge World History Volume II: A World with agriculture, 12,000 BCE–500 CE* (Cambridge Univ. Press, 2015).
- Cavalli-Sforza, L. L., Menozzi, P. & Piazza, A. *The History and Geography of Human Genes*. (Princeton Univ. Press, 1994).
- Gamba, C. et al. Genome flux and stasis in a five millennium transect of European prehistory. *Nat. Commun.* **5**, 5257 (2014).
- Pinhasi, R. et al. Optimal ancient DNA yields from the inner ear part of the human petrous bone. *PLoS One* **10**, e0129102 (2015).
- Fu, Q. et al. DNA analysis of an early modern human from Tianyuan Cave, China. *Proc. Natl. Acad. Sci. USA* **110**, 2223–2227 (2013).
- Fu, Q. et al. An early modern human from Romania with a recent Neanderthal ancestor. *Nature* **524**, 216–219 (2015).
- Haak, W. et al. Massive migration from the steppe was a source for Indo-European languages in Europe. *Nature* **522**, 207–211 (2015).
- Mathieson, I. et al. Genome-wide patterns of selection in 230 ancient Eurasians. *Nature* **528**, 499–503 (2015).
- Jones, E. R. et al. Upper Palaeolithic genomes reveal deep roots of modern Eurasians. *Nat. Commun.* **6**, 8912 (2015).
- Allentoft, M. E. et al. Population genomics of Bronze Age Eurasia. *Nature* **522**, 167–172 (2015).
- Fu, Q. et al. Genome sequence of a 45,000-year-old modern human from western Siberia. *Nature* **514**, 445–449 (2014).
- Günther, T. et al. Ancient genomes link early farmers from Atapuerca in Spain to modern-day Basques. *Proc. Natl. Acad. Sci. USA* (2015).
- Lazaridis, I. et al. Ancient human genomes suggest three ancestral populations for present-day Europeans. *Nature* **513**, 409–413 (2014).
- Olalde, I. et al. A common genetic origin for early farmers from Mediterranean Cardial and Central European LBK cultures. *Mol. Biol. Evol.* **32**, 3132–3142 (2015).
- Raghavan, M. et al. Upper Palaeolithic Siberian genome reveals dual ancestry of Native Americans. *Nature* **505**, 87–91 (2014).
- Patterson, N. et al. Ancient admixture in human history. *Genetics* **192**, 1065–1093 (2012).
- Patterson, N., Price, A. L. & Reich, D. Population structure and eigenanalysis. *PLoS Genet.* **2**, e190 (2006).
- Alexander, D. H., Novembre, J. & Lange, K. Fast model-based estimation of ancestry in unrelated individuals. *Genome Res.* **19**, 1655–1664 (2009).
- Prufer, K. et al. The complete genome sequence of a Neanderthal from the Altai Mountains. *Nature* **505**, 43–49 (2014).
- Meyer, M. et al. A high-coverage genome sequence from an archaic Denisovan individual. *Science* **338**, 222–226 (2012).
- Wall, J. D. et al. Higher levels of neanderthal ancestry in East Asians than in Europeans. *Genetics* **194**, 199–209 (2013).
- Green, R. E. et al. A draft sequence of the Neandertal genome. *Science* **328**, 710–722 (2010).
- Brace, C. L. et al. The questionable contribution of the Neolithic and the Bronze Age to European craniofacial form. *Proc. Natl. Acad. Sci. USA* **103**, 242–247 (2006).
- Ferembach, D. Squelettes du Natoufien d'Israël, étude anthropologique. *Anthropologie* **65**, 46–66 (1961).
- Fadhlaoui-Zid, K. et al. Genome-wide and paternal diversity reveal a recent origin of human populations in North Africa. *PLoS One* **8**, e80293 (2013).
- Henn, B. M. et al. Genomic ancestry of North Africans supports back-to-Africa migrations. *PLoS Genet.* **8**, e1002397 (2012).

- Bhatia, G., Patterson, N., Sankararaman, S. & Price, A. L. Estimating and interpreting FST: the impact of rare variants. *Genome Res.* **23**, 1514–1521 (2013).
- Fernández, E. et al. Ancient DNA analysis of 8000 B.C. near eastern farmers supports an early neolithic pioneer maritime colonization of Mainland Europe through Cyprus and the Aegean Islands. *PLoS Genet.* **10**, e1004401 (2014).
- Ammerman, A. J., Pinhasi, R. & Banffy, E. Comment on Ancient DNA from the first European farmers in 7500-year-old Neolithic sites. *Science* **312**, 1875; author reply 1875 (2006).
- Pagani, L. et al. Ethiopian genetic diversity reveals linguistic stratification and complex influences on the Ethiopian gene pool. *Am. J. Hum. Genet.* **91**, 83–96 (2012).
- Pickrell, J. K. et al. Ancient west Eurasian ancestry in southern and eastern Africa. *Proc. Natl. Acad. Sci. USA* **111**, 2632–2637 (2014).
- Keller, A. et al. New insights into the Tyrolean Iceman's origin and phenotype as inferred by whole-genome sequencing. *Nat. Commun.* **3**, 698 (2012).
- Moorjani, P. et al. Genetic evidence for recent population mixture in India. *Am. J. Hum. Genet.* **93**, 422–438 (2013).
- Reich, D., Thangaraj, K., Patterson, N., Price, A. L. & Singh, L. Reconstructing Indian population history. *Nature* **461**, 489–494 (2009).
- Fu, Q. et al. The genetic history of Ice Age Europe. *Nature* **534**, 200–205 (2016).

Supplementary Information is available in the online version of the paper.

Acknowledgements We thank the 238 human subjects who donated samples for genome-wide analysis, and D. Labuda and P. Zalloua for sharing samples from Poland and Lebanon. The Fig. 1a map was plotted in R using the worldHiRes map of the ‘mapdata’ package (using public domain data from the CIA World Data Bank II). We thank O. Bar-Yosef, M. Bonogofsky, I. Herskowitz, M. Lipson, I. Mathieson, H. May, R. Meadow, I. Olalde, S. Paabo, P. Skoglund, and N. Nakatsuka for comments and critiques, and D. Bradley, M. Dallakyan, S. Esayan, M. Ferry and M. Michel, and A. Yesayan, for contributions to bone preparation and ancient DNA work. D.F. and M.N. were supported by Irish Research Council grants GOIPG/2013/36 and GOIPD/2013/1, respectively. S.C. was funded by the Irish Research Council for Humanities and Social Sciences (IRCHSS) ERC Support Programme. Q.F. was funded by the Bureau of International Cooperation of the Chinese Academy of Sciences, the National Natural Science Foundation of China (L1524016) and the Chinese Academy of Sciences Discipline Development Strategy Project (2015-DX-C-03). The Scottish diversity data was funded by the Chief Scientist Office of the Scottish Government Health Directorates (CZD/16/6), the Scottish Funding Council (HR03006), and a project grant from the Scottish Executive Health Department, Chief Scientist Office (CZB/4/285). M.S., A.Tön., M.B. and P.K. were supported by the German Research Foundation (CRC 1052; B01, B03, C01). M.S.-P. was funded by a Wenner-Gren Foundation Dissertation Fieldwork grant (9005), and by the National Science Foundation DDRIG (BCS-1455744). P.K. was funded by the Federal Ministry of Education and Research, Germany (FKZ: 01EO1501). J.F.W. acknowledge the MRC ‘QTL in Health and Disease’ programme grant. The Romanian diversity data was supported by the EC Commission, Directorate General XII (Supplementary Agreement ERBICPDCT 940038 to the Contract ERBCHRXT 920032, coordinated by A. Piazza, Turin, Italy). M.R. received support from the Leverhulme Trust’s Doctoral Scholarship programme. O.S. and A.Tor. were supported by the University of Pavia (MIGRAT-IN-G) and the Italian Ministry of Education, University and Research: Progetti Ricerca Interesse Nazionale 2012. The Raqefet Cave Natufian project was supported by funds from the National Geographic Society (grant 8915-11), the Wenner-Gren Foundation (grant 7481) and the Irene Levi-Sala CARE Foundation, while radiocarbon dating on the samples was funded by the Israel Science Foundation (grant 475/10; E. Boaretto). R.P. was supported by ERC starting grant ADNABIOARC (263441). D.R. was supported by NIH grant GM100233, by NSF HOMINID BCS-1032255, and is a Howard Hughes Medical Institute investigator.

Author Contributions R.P. and D.R. conceived the idea for the study. D.N., G.R., D.C.M., S.C., S.A.R., G.L., F.B., B.Gas., J.M.M., M.G., V.E., A.M., C.M., F.G., N.A.H. and R.P. assembled skeletal material. N.R., D.F., M.N., B.Gam., K.Si., S.C., K.St., E.H., Q.F., G.G.-F., E.R.J., R.P. and D.R. performed or supervised ancient DNA wet laboratory work. L.B., M.B., A.C., G.C., D.C., P.F., E.G., S.M.K., P.K., J.K., D.M., M.M., D.A.M., S.O., M.B.R., O.S., M.S.-P., G.S., M.S., A.Tön., A.Tor., J.F.W., L.Y. and D.R. assembled present-day samples for genotyping. I.L., N.P. and D.R. developed methods for data analysis. I.L., S.M., Q.F., N.P. and D.R. analysed data. I.L., R.P. and D.R. wrote the manuscript and supplements.

Author Information The aligned sequences are available through the European Nucleotide Archive under accession number PRJEB14455. Fully public subsets of the analysis datasets are at http://genetics.med.harvard.edu/reichlab/Reich_Lab/Datasets.html. The complete dataset (including present-day humans for which the informed consent is not consistent with public posting of data) is available to researchers who send a signed letter to D.R. indicating that they will abide by specified usage conditions (Supplementary Information, section 2). Reprints and permissions information is available at www.nature.com/reprints. The authors declare no competing financial interests. Readers are welcome to comment on the online version of the paper. Correspondence and requests for materials should be addressed to I.L. (lazaridis@genetics.med.harvard.edu) or R.P. (ron.pinhasi@ucd.ie) or D.R. (reich@genetics.med.harvard.edu).

Reviewer Information *Nature* thanks O. Bar-Yosef, G. Coop and the other anonymous reviewer(s) for their contribution to the peer review of this work.

METHODS

No statistical methods were used to predetermine sample size. The experiments were not randomized and the investigators were not blinded to allocation during experiments and outcome assessment.

Ancient DNA data. In a dedicated ancient DNA laboratory at University College Dublin, we prepared powder from 132 ancient Near Eastern samples, either by dissecting the inner ear region of the petrous bone using a sandblaster (Renfert), or by drilling using a Dremel tool and single-use drill bits and selecting the best preserved bone fragments based on anatomical criteria. These fragments were then powdered using a mixer mill (Retsch Mixer Mill 400)⁴.

We performed all subsequent processing steps in a dedicated ancient DNA laboratory at Harvard Medical School, where we extracted DNA from the powder (usually 75 mg, range 14–81 mg) using an optimized ancient DNA extraction protocol³⁶, but replaced the assembly of Qiagen MinElute columns and extension reservoirs from Zymo Research with a High Pure Extender Assembly from the High Pure Viral Nucleic Acid Large Volume Kit (Roche Applied Science). We built a total of 170 barcoded double-stranded Illumina sequencing libraries for these samples³⁷, of which we treated 167 with uracil-DNA glycosylase (UDG) to remove the characteristic C-to-T errors of ancient DNA³⁸. The UDG treatment strategy is (by-design) inefficient at removing terminal uracils, allowing the mismatch rate to the human genome at the terminal nucleotide to be used for authentication³⁷. We updated this library preparation protocol in two ways compared to the original publication: first, we used 16U Bst2.0 Polymerase, Large Fragment (NEB) and 1× Isothermal amplification buffer (NEB) in a final volume of 25 µl fill-in reaction, and second, we used the entire inactivated 25 µl fill-in reaction in a total volume of 100 µl PCR mix with 1 µM of each primer³⁹. We included extraction negative controls (where no sample powder was used) and library negative controls (where extract was supplemented by water) in every batch of samples processed and carried them through the entire wet laboratory processing to test for reagent contamination.

We screened the libraries by hybridizing them in solution to a set of oligonucleotide probes tiling the mitochondrial genome⁴⁰, using the protocol described previously⁷. We sequenced the enriched libraries using an Illumina NextSeq 500 instrument using 2× 76 bp reads, trimmed identifying sequences (seven base pair molecular barcodes at either end) and any trailing adapters, merged read pairs that overlapped by at least 15 base pairs, and mapped the merged sequences to the RSRs mitochondrial DNA reference genome⁴¹, using the Burrows Wheeler Aligner⁴² (*bwa*) and the command *samse* (v0.6.1).

We enriched promising libraries for a targeted set of ~1.2 million SNPs⁸ as in ref. 5, and adjusted the blocking oligonucleotide and primers to be appropriate for our libraries. The specific probe sequences are given in supplementary data 2 of ref. 7, and supplementary data 1 of ref. 6. We sequenced the libraries on an Illumina NextSeq 500 using 2× 76 bp reads. We trimmed identifying sequences (molecular barcodes) and any trailing adapters, merged pairs that overlapped by at least 15 base pairs (allowing up to one mismatch), and mapped the merged sequences to *hg19* using the single-ended aligner *samse* in *bwa* (v0.6.1). We removed duplicated sequences by identifying sets of sequences with the same orientation and start and end positions after alignment to *hg19*; we picked the highest quality sequence to represent each set. For each sample, we represented each SNP position by a randomly chosen sequence, restricting to sequences with a minimum mapping quality (MAPQ ≥ 10), sites with a minimum sequencing quality (≥20), and removing two bases at the ends of reads. We sequenced the enriched products up to the point that we estimated that generating a hundred new sequences was expected to add data on less than about one new SNP⁸.

Testing for contamination and quality control. For each ancient DNA library, we evaluated authenticity in several ways. First, we estimated the rate of matching to the consensus sequence for mitochondrial genomes sequenced to a coverage of at least tenfold from the initial screening data. Of the 76 libraries that contributed to our dataset (coming from 45 samples), 70 had an estimated rate of sequencing matching to the consensus of >95% according to contamMix⁵ (the remaining libraries had estimated match rates of 75–92%, but gave no sign of being outliers in principal component analysis or X-chromosome contamination analysis so we retained them for analysis) (Supplementary Table 1). We quantified the rate of C-to-T substitution in the final nucleotide of the sequences analysed, relative to the human reference genome sequence, and found that all the libraries analysed had rates of at least 3% (ref. 37), consistent with genuine ancient DNA. For the nuclear data from males, we used the ANGSD software⁴³ to obtain a conservative X-chromosome estimate of contamination. We determined that all libraries that passed our quality control and for which we had sufficient X-chromosome data to make an assessment, had contamination rates of 0–1.5%. Finally, we merged data for samples for which we had multiple libraries to produce an analysis dataset. **Affymetrix Human Origins genotyping data.** We genotyped 238 present-day individuals from 17 diverse West Eurasian populations on the Affymetrix Human Origins array¹⁶, and applied quality control analyses as previously described¹³

(Supplementary Table 2). We merged the newly generated data with data from 2,345 individuals previously genotyped on the same array¹³. All individuals that were genotyped provided individual informed consent consistent with studies of population history, following protocols approved by the ethical review committees of the institutions of the researchers who collected the samples. The collection and analysis of genome-wide data on anonymized samples at Harvard Medical School for the purpose of studying population history was approved by the Harvard Human Research Protection Program, protocol 11681, re-reviewed on 12 July 2016. Anonymized aliquots of DNA from all individuals were sent to the core facility of the Center for Applied Genomics at the Children's Hospital of Philadelphia for genotyping and data processing. For 127 of the individuals with newly reported data, the informed consent was consistent with public distribution of data, and the data can be downloaded at http://genetics.med.harvard.edu/reich/Reich_Lab/Datasets.html. To access data for the remaining 111 newly reported samples, researchers should send a signed letter to D.R. containing the following text: “(a) I will not distribute the data outside my collaboration; (b) I will not post the data publicly; (c) I will make no attempt to connect the genetic data to personal identifiers for the samples; (d) I will use the data only for studies of population history; (e) I will not use the data for any selection studies; (f) I will not use the data for medical or disease-related analyses; (g) I will not use the data for commercial purposes.” Supplementary Table 2 specifies which samples are consistent with which type of data distribution.

Datasets. We carried out population genetic analysis on two datasets: (i) *HO* includes 2,583 present-day humans genotyped on the Human Origins array^{13,16} including 238 newly reported, (Supplementary Table 2; Supplementary Information, section 2), and 281 ancient individuals on a total of 592,146 autosomal SNPs. (ii) *HOII* includes the 281 ancient individuals on a total of 1,055,186 autosomal SNPs, including those present in both the Human Origins and Illumina genotyping platforms, but excluding SNPs on the sex chromosomes or additional SNPs of the 1,240k capture array that were included because of their potential functional importance⁸. We used *HO* for analyses that involve both ancient and present-day individuals, and *HOII* for analysis on ancient individuals alone. We also used 235 individuals from Pagani *et al.*³⁰ genotyped at 418,700 autosomal SNPs to study admixture in East Africans (Supplementary Information, section 8). Ancient individuals are represented in ‘pseudo-haploid’ form by randomly choosing one allele for each position of the array.

Principal components analysis. We carried out principal components analysis in the *smartpca* program of EIGENSOFT¹⁷, using default parameters and the lsqproject: YES¹³ and numoutlieriter: 0 options. We carried out PCA on the *HO* dataset for 991 present-day West Eurasians (Extended Data Fig. 1), and projected the 278 ancient individuals (Fig. 1b).

ADMIXTURE analysis. We carried out ADMIXTURE analysis¹⁸ of the *HO* dataset after pruning for linkage disequilibrium in PLINK^{44,45} with parameters indep-pairwise 200 25 0.4, which retained 296,309 SNPs. We performed analysis in 20 replicates with different random seeds, and retained the highest likelihood replicate for each value of *K*. We show the *K*=11 results for the 281 ancient samples in Extended Data Fig. 2a (this is the lowest *K* for which components maximized in European hunter-gatherers, ancient Levant, and ancient Iran appear).

f-statistics. We carried out analysis of *f*₃-statistics, *f*₄-ratio, and *f*₄-statistics statistics using the ADMIXTOOLS¹⁶ programs *qp3Pop*, *qpF4ratio* with default parameters, and *qpDstat* with f4mode: YES, and computed standard errors with a block jack-knife⁴⁶. For computing *f*₃-statistics with an ancient population as a target, we set the inbreed: YES parameter. We computed *f*-statistics on the *HOII* dataset when no present-day humans were involved and on the *HO* dataset when they were. We computed the statistic *f*₄(*Test*, Mbuti; Altai, Denisovan) in Fig. 2 on the *HOII* dataset after merging with whole genome data on 3 Mbuti individuals from Panel C of the Simons Genome Diversity Project⁴⁷. We computed the dendrogram of Extended Data Fig. 3 showing hierarchical clustering of populations with outgroup *f*₃-statistics using the open source *heatmap.2* function of the *gplots* package in R.

Negative correlation of Basal Eurasian ancestry with Neanderthal ancestry. We used the *lm* function of R to fit a linear regression of the rate of allele sharing of a *Test* population with the Altai Neanderthal as measured by *f*₄(*Test*, Mbuti; Altai, Denisovan) as the dependent variable, and the proportion of Basal Eurasian ancestry (Supplementary Information, section 4) as the predictor variable. Extrapolating from the fitted line, we obtain the value of the statistic expected if *Test* is a population of 0% or 100% Basal Eurasian ancestry. We then compute the ratio of the Neanderthal ancestry estimate in Basal Eurasians relative to non-Basal Eurasians as *f*₄(100% Basal Eurasian, Mbuti; Altai, Denisovan)/*f*₄(0% Basal Eurasian, Mbuti; Altai, Denisovan). We use a block jack-knife⁴⁶, dropping one of 100 contiguous blocks of the genome at a time, to estimate the value and standard error of this quantity (9 ± 26%). We compute a 95% confidence interval based on the point estimate ± 1.96-times the standard error: −42 to 60%. We truncated to 0–60%

on the assumption that Basal Eurasians had no less Neanderthal admixture than Mbuti from sub-Saharan Africa.

Estimation of F_{ST} coefficients. We estimated F_{ST} in *smartpca*¹⁷ with default parameters, inbreed: YES, and fstonly: YES.

Admixture graph modelling. We carried out Admixture Graph modelling with the *qpGraph* software¹⁶ using Mbuti as an outgroup unless otherwise specified.

Testing for the number of streams of ancestry. We used the *qpWave*^{33,48} software, described in Supplementary Information, section 10 of ref. 7, to test whether a set of ‘Left’ populations is consistent with being related via as few as N streams of ancestry to a set of ‘Right’ populations by studying statistics of the form $X(u, v) = F_4(u_0, u; v_0, v)$ where u_0, v_0 are basis populations chosen from the ‘Left’ and ‘Right’ sets and u, v are other populations from these sets. We use a Hotelling’s T^2 test⁴⁸ to evaluate whether the matrix of size $(L-1)*(R-1)$, where L, R are the sizes of the ‘Left’ and ‘Right’ sets has rank m . If this is the case, we can conclude that the ‘Left’ set is related via at least $N = m+1$ streams of ancestry differently to the ‘Right’ set. We use the parameter allsnps: YES which computes each f_4 -statistic based on the full set of SNPs with coverage among the four populations used in the statistic (without regard to whether the SNPs are covered in the other populations in the ‘Left’ and ‘Right’ sets).

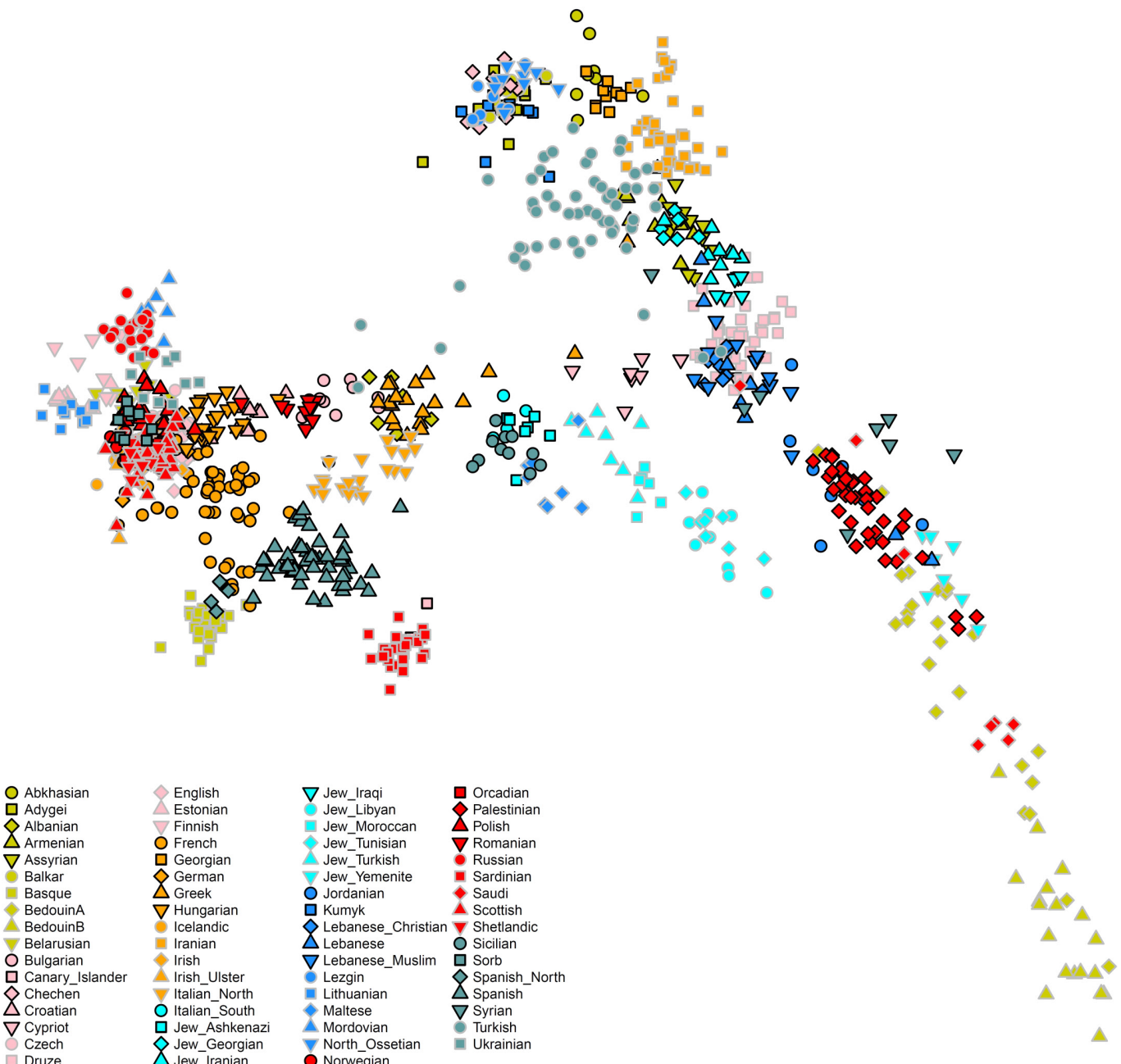
Inferring mixture proportions without an explicit phylogeny. We used the *qpAdm* methodology described in Supplementary Information, section 10 of ref. 7 to estimate the proportions of ancestry in a *Test* population deriving from a mixture of N ‘reference’ populations by exploiting (but not explicitly modelling) shared genetic drift with a set of ‘Outgroup’ populations (Supplementary Information, section 7). We set the details: YES parameter, which reports a normally distributed Z-score estimated with a block jack-knife for the difference between the statistics $f_4(u_0, \text{Test}; v_0, v)$ and $f_4(u_0, \text{Estimated Test}; v_0, v)$ where *Estimated Test* is $\sum_{i=1}^N \alpha_i f_4(u_0, \text{Ref}_i; v_0, v)$, the average of these f_4 -statistics weighed by the mixture proportions α_i from the N reference populations. We use the allsnps: YES parameter.

Modelling admixture from ghost populations. We model admixture from a ‘ghost’ (unobserved) population X in the specific case that X has part of its ancestry from two unobserved ancestral populations p and q . Any population X composed

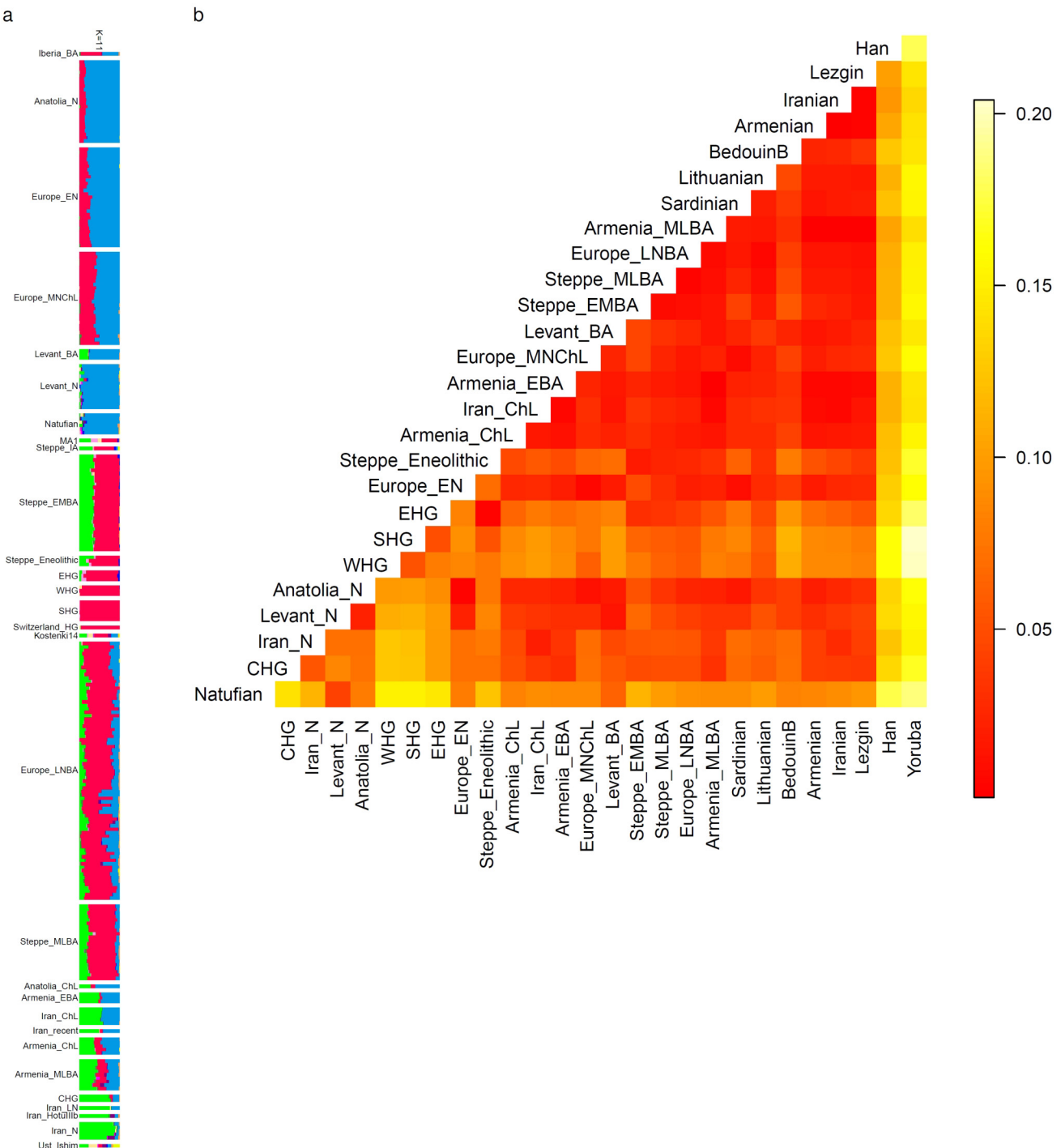
of the same populations p and q resides on a line defined by two observed reference populations r_1 and r_2 composed of the same elements p and q according to a parametric equation $x = r_1 + \lambda(r_2 - r_1)$ with real-valued parameter λ . We define and solve the optimization problem of fitting λ and obtain mixture proportions (Supplementary Information, section 10).

Code availability. Code implementing the newly developed method for modelling admixture from ghost populations is available on request from I.L.

36. Dabney, J. *et al.* Complete mitochondrial genome sequence of a Middle Pleistocene cave bear reconstructed from ultrashort DNA fragments. *Proc. Natl. Acad. Sci. USA* **110**, 15758–15763 (2013).
37. Rohland, N., Harney, E., Mallick, S., Nordenfelt, S. & Reich, D. Partial uracil-DNA-glycosylase treatment for screening of ancient DNA. *Phil. Trans. R. Soc. Lond. B* **370**, 20130624 (2015).
38. Briggs, A. W. *et al.* Removal of deaminated cytosines and detection of in vivo methylation in ancient DNA. *Nucleic Acids Res.* **38**, e87 (2010).
39. Korlević, P. *et al.* Reducing microbial and human contamination in DNA extractions from ancient bones and teeth. *Biotechniques* **59**, 87–93 (2015).
40. Meyer, M. *et al.* A mitochondrial genome sequence of a hominin from Sima de los Huesos. *Nature* **505**, 403–406 (2014).
41. Behar, D. M. *et al.* A “Copernican” reassessment of the human mitochondrial DNA tree from its root. *Am. J. Hum. Genet.* **90**, 675–684 (2012).
42. Li, H. & Durbin, R. Fast and accurate short read alignment with Burrows-Wheeler transform. *Bioinformatics* **25**, 1754–1760 (2009).
43. Korneliussen, T. S., Albrechtsen, A. & Nielsen, R. ANGSD: Analysis of next generation sequencing data. *BMC Bioinformatics* **15**, 356 (2014).
44. Purcell, S. *et al.* PLINK: a tool set for whole-genome association and population-based linkage analyses. *Am. J. Hum. Genet.* **81**, 559–575 (2007).
45. Chang, C. C. *et al.* Second-generation PLINK: rising to the challenge of larger and richer datasets. *Gigascience* **4**, 7 (2015).
46. Busing, F. T. A., Meijer, E. & Leeden, R. Delete-m Jackknife for Unequal m. *Stat. Comput.* **9**, 3–8 (1999).
47. Sudmant, P. H. *et al.* Global diversity, population stratification, and selection of human copy-number variation. *Science* **349**, aab3761 (2015).
48. Reich, D. *et al.* Reconstructing Native American population history. *Nature* **488**, 370–374 (2012).
49. Gallego Llorente, M. *et al.* Ancient Ethiopian genome reveals extensive Eurasian admixture in Eastern Africa. *Science* **350**, 820–822 (2015).

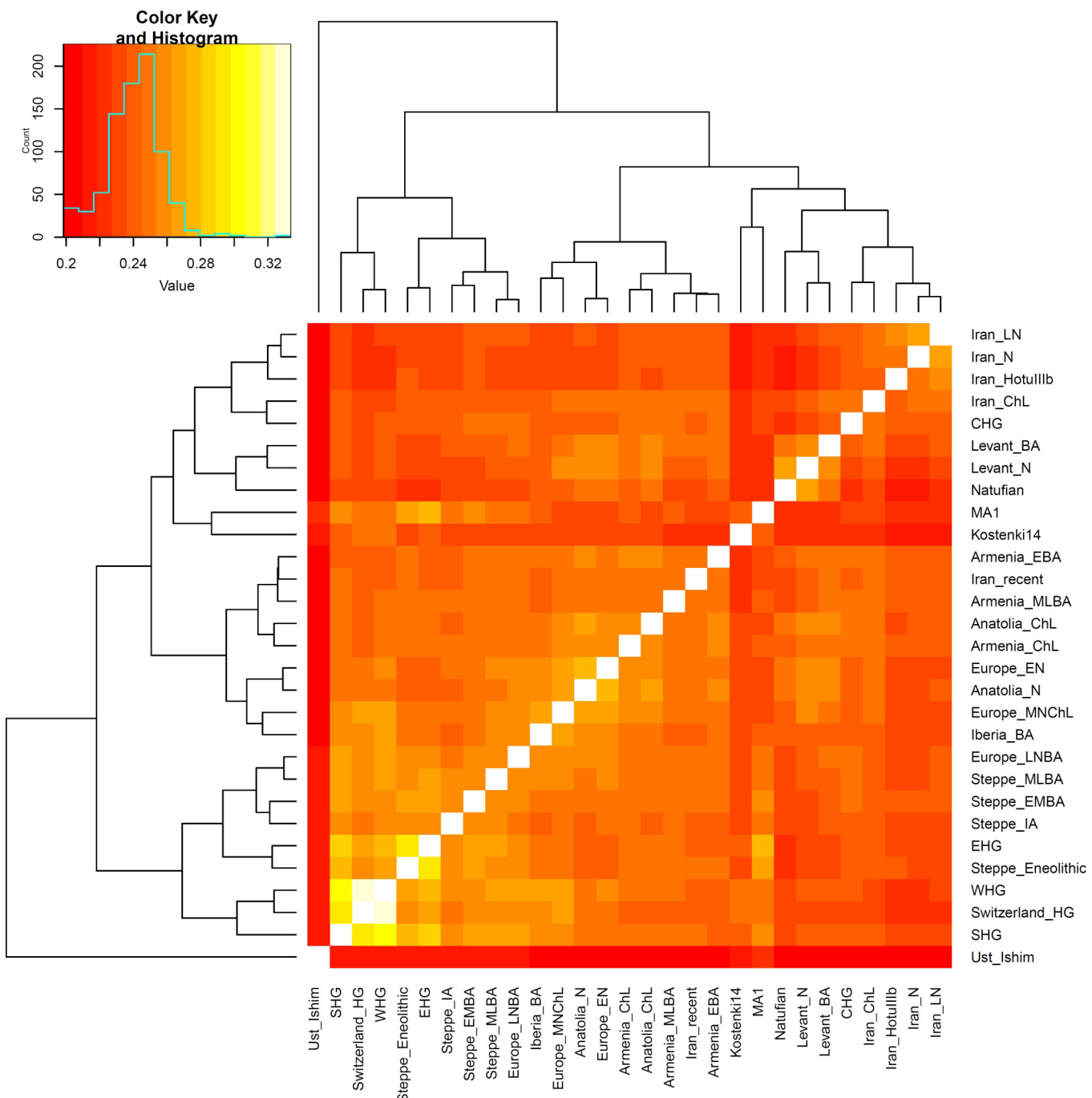


Extended Data Figure 1 | Principal components analysis of 991 present-day West Eurasians. The PCA analysis is performed on the same set of individuals as are reported in Fig. 1b, using EIGENSOFT. Here, we colour the samples by population (to highlight the present-day populations) instead of using grey points as in Fig. 1b (where the goal is to highlight ancient samples).



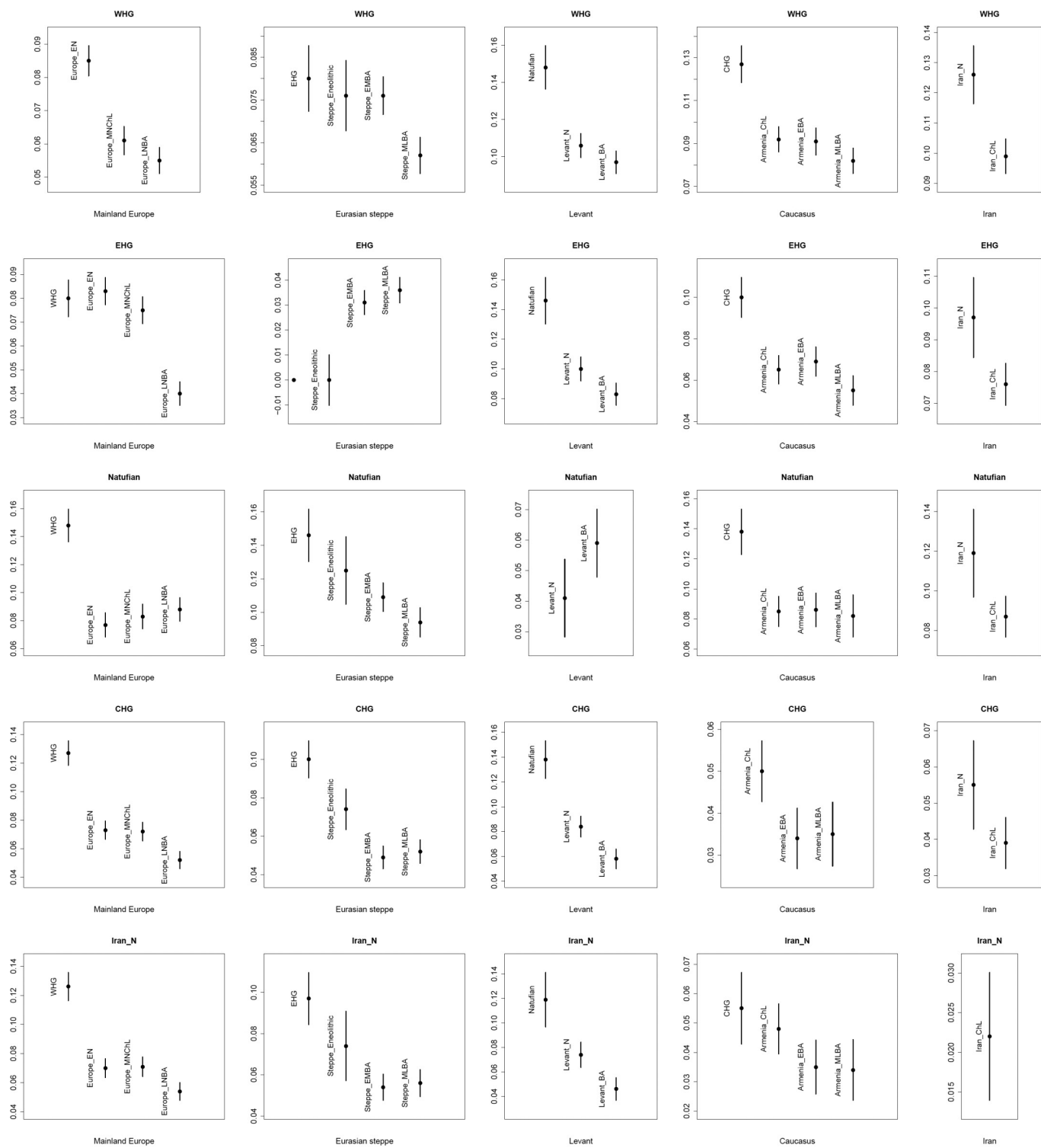
Extended Data Figure 2 | Genetic structure in ancient West Eurasian populations across time and decline of genetic differentiation over time. **a**, ADMIXTURE model-based clustering analysis of 2,583 present-day humans and 281 ancient samples; we show the results only for ancient

samples for $K = 11$ clusters. **b**, Pairwise F_{ST} between 19 Ancient West Eurasian populations (arranged in approximate chronological order), and select present-day populations.

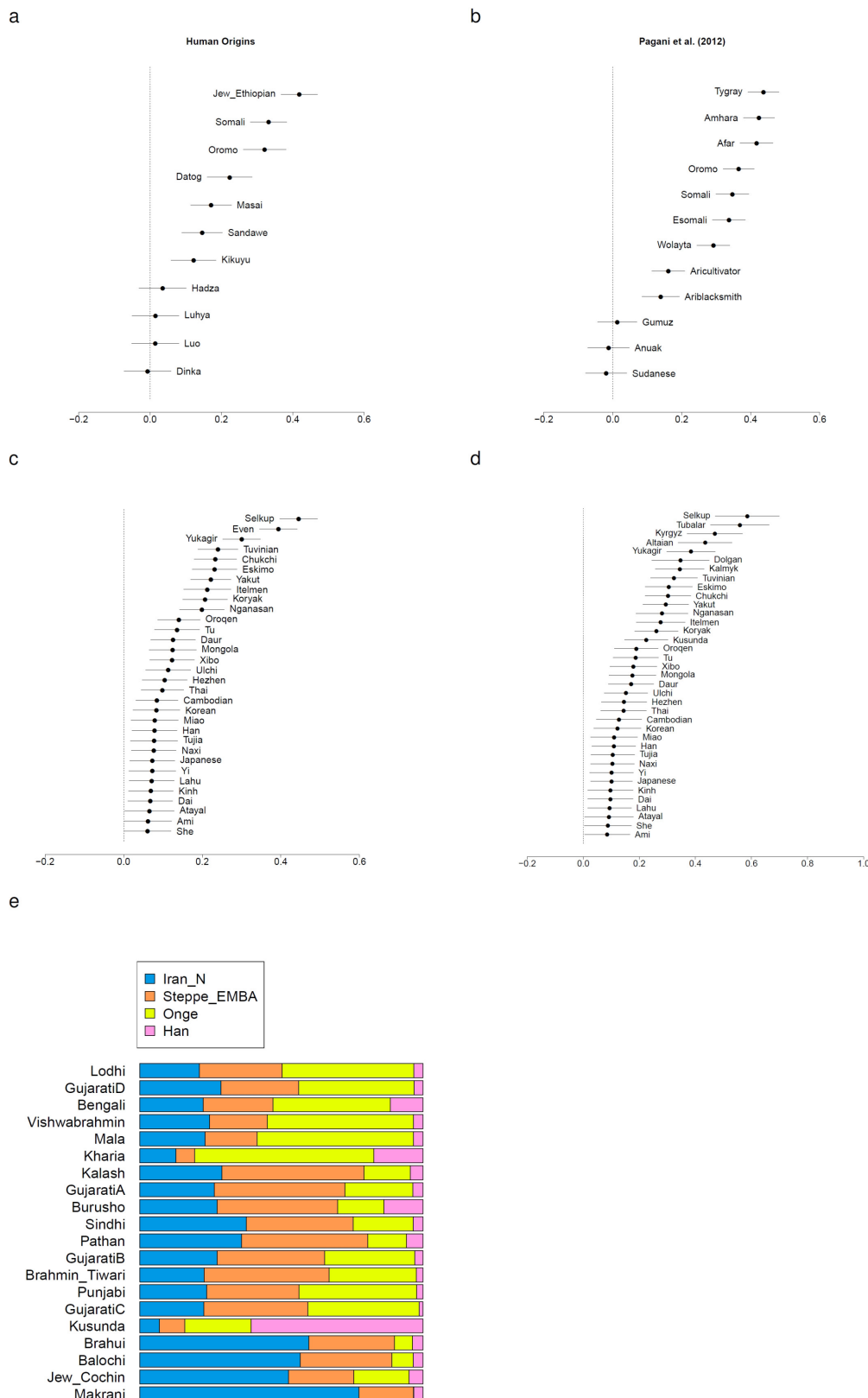


Extended Data Figure 3 | Outgroup $f_3(\text{Mbuti}; X, Y)$ for pairs of ancient populations. The dendrogram is plotted for convenience and should not be interpreted as a phylogenetic tree. Areas of high shared genetic drift are 'yellow' and include from top-right to bottom-left along the diagonal:

early Anatolian and European farmers; European hunter-gatherers, Steppe populations and populations admixed with steppe ancestry; populations from the Levant from the Epipalaeolithic (Natufians) to the Bronze Age; populations from Iran from the Mesolithic to the Late Neolithic.



Extended Data Figure 4 | Reduction of genetic differentiation in West Eurasia over time. We measure differentiation by F_{ST} . Each column of the 5×5 matrix of plots represents a major region and each row the earliest population with at least two individuals from each major region.



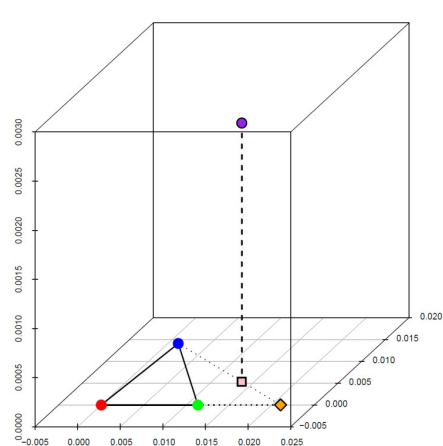
Extended Data Figure 5 | West Eurasian related admixture in East Africa, Eastern Eurasia and South Asia. **a**, Levantine ancestry in Eastern Africa in the Human Origins dataset. **b**, Levantine ancestry in different Eastern African population in the dataset from Pagani *et al.* (2012); the remainder of the ancestry is a clade with Mota, a ~4,500 year old sample

from Ethiopia⁴⁹. **c**, EHG ancestry in Eastern Eurasians. **d**, Afontova Gora (AG2)-related ancestry in Eastern Eurasians; the remainder of their ancestry is a clade with Onge. **e**, Mixture proportions for South Asian populations showing that they can be modelled as having West Eurasian-related ancestry similar to that in populations from both the Eurasian steppe and Iran.

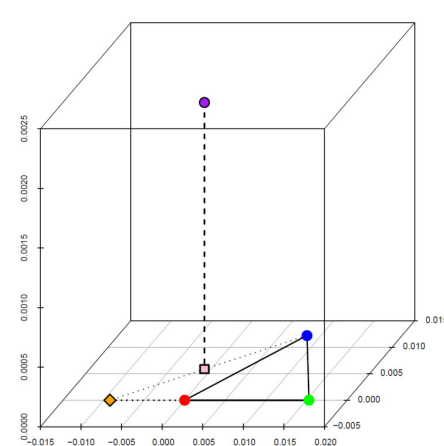


Extended Data Figure 6 | Inferred position of ancient populations in West Eurasian PCA according to the model of Fig. 4.

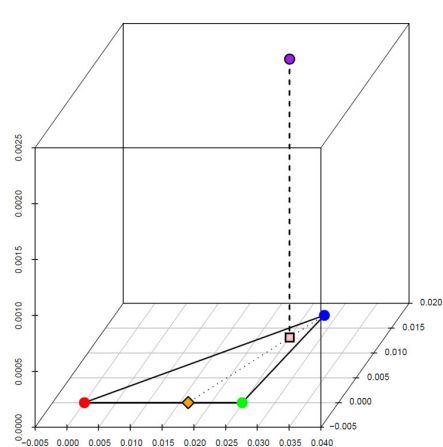
a



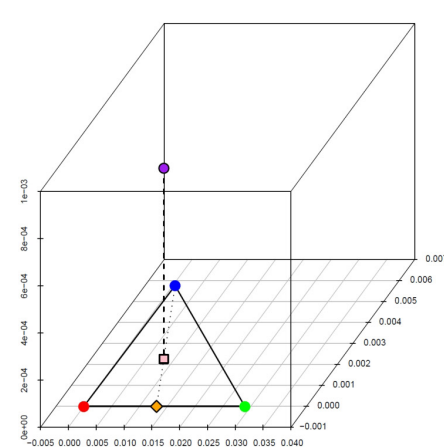
b



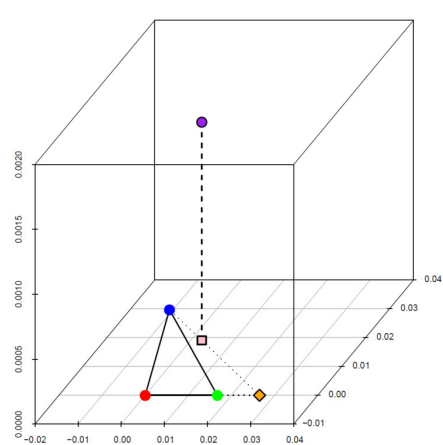
c



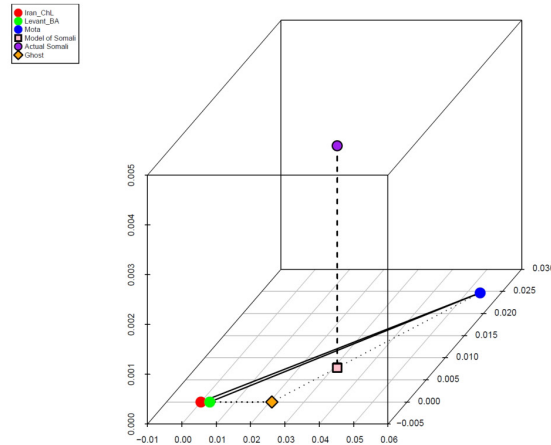
d



e

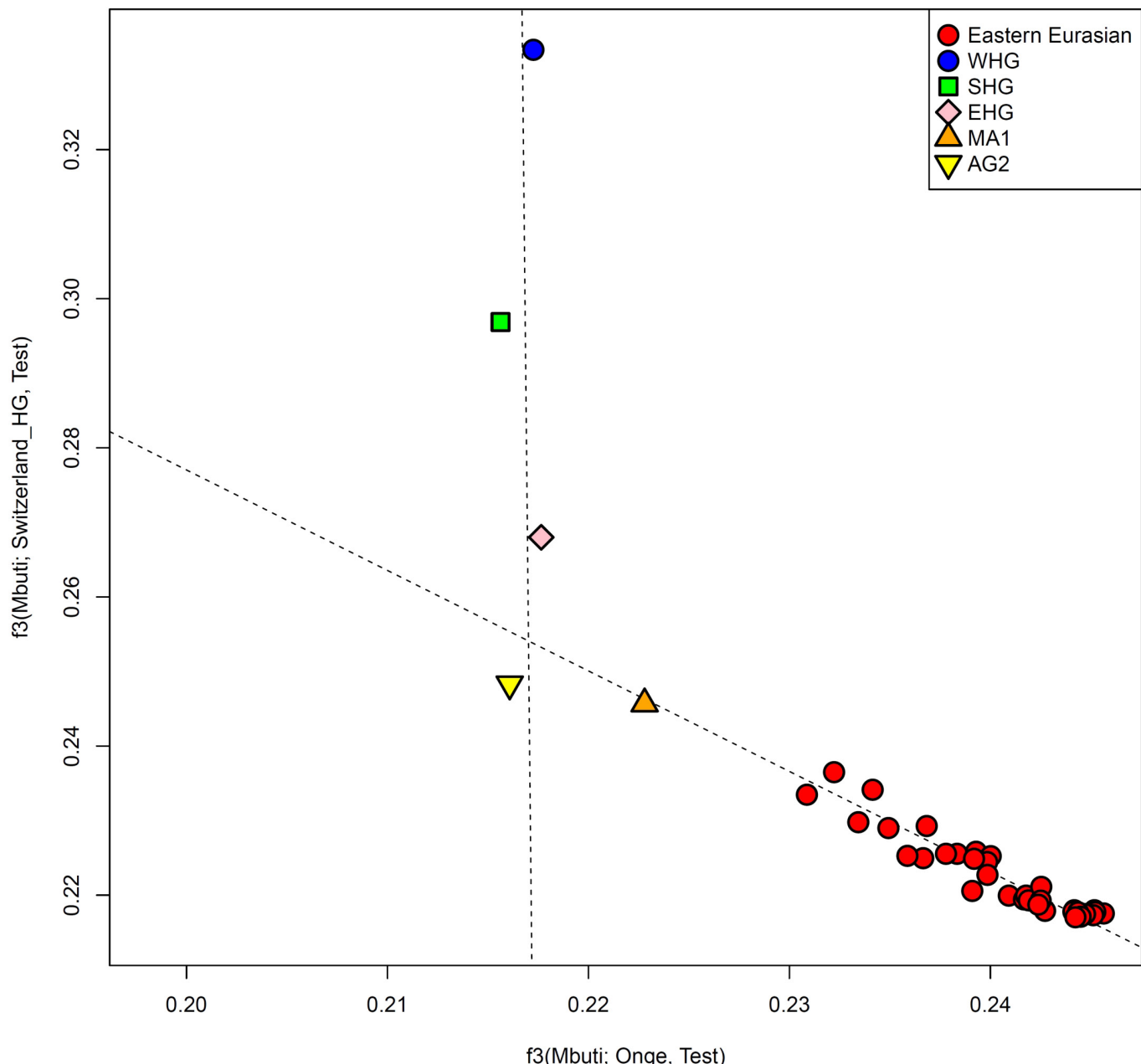


f



Extended Data Figure 7 | Admixture from ghost populations using ‘cline intersection’. **a–f**, We model each *Test* population (purple) as a mixture (pink) of a fixed reference population (blue) and a ghost population (orange) residing on the cline defined by two other populations (red and green) according to the visualization method of Supplementary Information, section 10. **a**, Early/Middle Bronze Age steppe populations are a mixture of Iran_ChL and a population on the WHG→SHG cline. **b**, Scandinavian hunter-gatherers (SHG) are a mixture of WHG and a

population on the Iran_ChL→Steppe_EMBA cline. **c**, Caucasus hunter-gatherers (CHG) are a mixture of Iran_N and both WHG and EHG. **d**, Late Neolithic/Bronze Age Europeans are a mixture of the preceding Europe_MNChL population and a population with both EHG and Iran_ChL ancestry. **e**, Somalis are a mixture of Mota⁴⁹ and a population on the Iran_ChL→Levant_BA cline. **f**, Eastern European hunter-gatherers (EEHG) are a mixture of WHG and a population on the Onge→Han cline.



Extended Data Figure 8 | Admixture from a ‘ghost’ ANE population into both European and Eastern Eurasian ancestry. EHG, and Upper Palaeolithic Siberians Mal’ta 1 (MA1) and Afontova Gora 2 (AG2) are positioned near the intersection of clines formed by European

hunter-gatherers (WHG, SHG, EHG) and Eastern non-Africans in the space of outgroup f_3 -statistics of the form $f_3(\text{Mbuti}; \text{Papuan}, \text{Test})$ and $f_3(\text{Mbuti}; \text{Switzerland}_\text{HG}, \text{Test})$.

Extended Data Table 1 | No evidence for admixture related to sub-Saharan Africans in Natufians

Other Ancient	African	$f_4(\text{Natufian}, \text{Other Ancient}; \text{African}, \text{Chimp})$	Z	Number of SNPs
EHG	Mbuti	-0.00044	-1.0	254033
EHG	Yoruba	0.00029	0.7	254033
EHG	Ju_hoan_North	-0.00015	-0.4	254033
EHG	Mota	-0.00022	-0.4	253986
WHG	Mbuti	-0.00067	-1.7	261514
WHG	Yoruba	-0.00045	-1.1	261514
WHG	Ju_hoan_North	-0.00046	-1.2	261514
WHG	Mota	-0.00129	-2.3	261461
SHG	Mbuti	-0.00076	-2.0	255686
SHG	Yoruba	-0.00039	-1.0	255686
SHG	Ju_hoan_North	-0.00052	-1.4	255686
SHG	Mota	-0.00091	-1.7	255641
Switzerland_HG	Mbuti	-0.00018	-0.4	261322
Switzerland_HG	Yoruba	0.00019	0.4	261322
Switzerland_HG	Ju_hoan_North	0.00009	0.2	261322
Switzerland_HG	Mota	-0.00062	-0.9	261276
Kostenki14	Mbuti	0.00034	0.7	246765
Kostenki14	Yoruba	0.00120	2.3	246765
Kostenki14	Ju_hoan_North	0.00069	1.4	246765
Kostenki14	Mota	0.00036	0.5	246719
MA1	Mbuti	-0.00038	-0.7	191819
MA1	Yoruba	0.00009	0.2	191819
MA1	Ju_hoan_North	-0.00010	-0.2	191819
MA1	Mota	-0.00038	-0.5	191782
CHG	Mbuti	-0.00051	-1.2	261505
CHG	Yoruba	-0.00012	-0.3	261505
CHG	Ju_hoan_North	-0.00013	-0.3	261505
CHG	Mota	-0.00042	-0.7	261456
Iran_N	Mbuti	-0.00018	-0.4	232927
Iran_N	Yoruba	0.00036	0.8	232927
Iran_N	Ju_hoan_North	0.00041	0.9	232927
Iran_N	Mota	0.00006	0.1	232880

We computed the statistic $f_4(\text{Natufian}, \text{Other Ancient}; \text{African}, \text{Chimp})$ varying *African* to be Mbuti, Yoruba, Ju_hoan_North, or the ancient Mota individual. Gene flow between Natufians and African populations would be expected to bias these statistics positive. However, we find most of them to be negative in sign and all of them to be non-significant ($|Z| < 3$), providing no evidence that Natufians differ from other ancient samples with respect to African populations.

Extended Data Table 2 | Admixture f_3 -statistics

Test	Reference ₁	Reference ₂	f_3 (Test; Reference ₁ , Reference ₂)	Z-score	Number of SNPs
Anatolia_N	Iberia_BA	Levant_N	-0.00034	-0.2	111632
Armenia_ChL	EHG	Levant_N	-0.00249	-1.5	167020
Armenia_EBA	Anatolia_N	CHG	-0.01017	-7.9	195596
Armenia_MLBA	Anatolia_N	Steppe_EMBA	-0.00809	-7.3	203796
CHG	Anatolia_ChL	Iran_HotuIIb	0.02612	3.6	9884
EHG	Steppe_Eneolithic	Switzerland_HG	-0.00282	-0.9	67938
Europe_EN	Anatolia_N	WHG	-0.00494	-11.2	380684
Europe_LNBA	Europe_MNChL	Steppe_EMBA	-0.00920	-41.8	414782
Europe_MNChL	Anatolia_N	WHG	-0.01351	-26.8	363672
Iran_ChL	Anatolia_N	Iran_N	-0.01285	-10.6	167941
Iran_N	Iran_LN	Gana	-0.00462	-1.1	17804
Levant_BA	Iran_N	Levant_N	-0.00853	-4.7	118269
Levant_N	Europe_MNChL	Natufian	-0.00671	-3.6	61845
Natufian	Iberia_BA	Iran_HotuIIb	0.07613	3.4	1054
SHG	Steppe_Eneolithic	Switzerland_HG	0.00728	3.2	154825
Steppe_EMBA	EHG	Abkhasian	-0.00756	-11.2	349359
Steppe_Eneolithic	EHG	Iran_LN	-0.01637	-4.2	25100
Steppe_MLBA	Europe_MNChL	Steppe_EMBA	-0.00573	-18.0	378298
WHG	Switzerland_HG	Saudi	-0.01562	-7.7	218758
Abkhasian	CHG	Sardinian	-0.00754	-13.1	387956
Adygei	Anatolia_N	Eskimo	-0.00699	-14.4	413128
Albanian	Europe_EN	Burusho	-0.00650	-16.8	395851
Armenian	Anatolia_N	Sindhi	-0.00603	-19.5	406021
Assyrian	Iran_N	Sardinian	-0.00672	-11.8	309055
Balkar	Anatolia_N	Chukchi	-0.00975	-18.8	401928
Basque	Switzerland_HG	Druze	-0.00726	-12.6	416070
BedouinA	Europe_EN	Yoruba	-0.01584	-42.8	460762
BedouinB	Iran_HotuIIb	Natufian	0.01384	4.1	32266
Belarusian	WHG	Iranian	-0.00974	-19.8	392363
Bulgarian	Anatolia_N	Steppe_EMBA	-0.00807	-26.7	400263
Canary_Islander	Europe_MNChL	Mende	-0.00829	-5.9	353172
Chechen	Anatolia_N	Eskimo	-0.00440	-7.9	396678
Croatian	WHG	Druze	-0.00871	-18.6	394032
Cypriot	Anatolia_N	Sindhi	-0.00562	-16.1	401141
Czech	SHG	Druze	-0.00919	-21.7	374705
Druze	Iran_N	Sardinian	-0.00269	-5.8	343813
English	Steppe_EMBA	Sardinian	-0.00628	-20.6	402502
Estonian	SHG	Druze	-0.00789	-17.6	371575
Finnish	SHG	Assyrian	-0.00716	-12.6	355744
French	Steppe_EMBA	Sardinian	-0.00669	-37.9	441807
Georgian	CHG	Sardinian	-0.00782	-13.7	390744
German	WHG	Druze	-0.01103	-22.9	391302
Greek	Europe_EN	Pathan	-0.00600	-30.0	421984
Hungarian	Steppe_EMBA	Sardinian	-0.00644	-31.2	420017
Icelandic	WHG	Abkhasian	-0.00974	-17.0	394625
Iranian	Anatolia_N	Sindhi	-0.00594	-30.9	443011
Irish	Steppe_EMBA	Sardinian	-0.00590	-22.8	416663
Irish_Ulster	SHG	Assyrian	-0.00909	-15.6	350547
Italian_North	Europe_EN	Steppe_EMBA	-0.00627	-26.4	419169
Italian_South	Iberia_BA	Iran_HotuIIb	0.01224	2.6	17678
Jew_Ashkenazi	Anatolia_N	Koryak	-0.00532	-9.4	389012
Jew_Georgian	Iran_N	Sardinian	-0.00306	-4.2	292410
Jew_Iranian	Iran_N	Sardinian	-0.00385	-5.8	302446
Jew_Iraqi	Iran_N	Sardinian	-0.00486	-6.5	287673
Jew.Libyan	Europe_EN	Yoruba	-0.00397	-7.2	415797
Jew_Moroccan	Europe_EN	Yoruba	-0.00649	-10.9	405193
Jew_Tunisian	Anatolia_N	Mende	-0.00276	-4.1	399354
Jew_Turkish	Anatolia_N	Burusho	-0.00571	-16.4	405254
Jew_Yemenite	Natufian	Kalash	-0.00341	-3.8	174052
Jordanian	Europe_EN	Yoruba	-0.01283	-26.7	423649
Kumyk	Anatolia_N	Chukchi	-0.01025	-19.6	396439
Lebanese	Anatolia_N	Yoruba	-0.01022	-19.5	414854
Lebanese_Christian	Anatolia_N	Sindhi	-0.00504	-15.7	404858
Lebanese_Muslim	Anatolia_N	Brahmin_Tiwari	-0.00616	-20.4	415129
Lezgin	Steppe_EMBA	Jew_Yemenite	-0.00481	-13.1	398974
Lithuanian	WHG	Abkhasian	-0.00999	-17.7	386718
Maltese	Anatolia_N	Brahmin_Tiwari	-0.00518	-14.5	404438
Mordovian	WHG	Iranian	-0.00912	-18.4	395230
North_Osetian	Anatolia_N	Chukchi	-0.00894	-17.2	401729
Norwegian	WHG	Abkhasian	-0.00957	-16.5	393546
Orcadian	SHG	Druze	-0.00662	-15.8	379656
Palestinian	Europe_EN	Yoruba	-0.01129	-31.3	464066
Polish	SHG	Druze	-0.00924	-27.8	394654
Romanian	Europe_EN	Steppe_EMBA	-0.00549	-16.9	397119
Russian	SHG	Turkish	-0.00731	-25.0	398393
Sardinian	Anatolia_N	Switzerland_HG	-0.00587	-9.6	417931
Saudi	Anatolia_N	Dinka	-0.00326	-5.1	404923
Scottish	Steppe_EMBA	Sardinian	-0.00622	-26.6	426660
Shetlandic	WHG	Abkhasian	-0.00868	-14.6	386562
Sicilian	Anatolia_N	Brahmin_Tiwari	-0.00646	-22.2	411481
Sorb	SHG	Palestinian	-0.00787	-16.8	366924
Spanish	Steppe_EMBA	Sardinian	-0.00557	-32.2	447735
Spanish_North	WHG	Armenian	-0.00825	-10.9	356832
Syrian	Europe_EN	Dinka	-0.01002	-17.3	410920
Turkish	Europe_EN	Sindhi	-0.00709	-41.1	448975
Ukrainian	WHG	Abkhasian	-0.01183	-21.4	388282

We show the lowest Z-score of the statistic $f_3(\text{Test}; \text{Reference}_1, \text{Reference}_2)$ for Test populations with at least 2 individuals and every pair ($\text{Reference}_1, \text{Reference}_2$) of ancient or present-day source populations. Z-scores lower than -3 are highlighted and indicate that the Test population is admixed from sources related to (but not identical to) the reference populations. Z-scores greater than -3 are consistent with the population either being admixed or not.